^{14}N NMR study of the glass transition in $(NH_4I)_{0.44}(KI)_{0.56}$

R. Blinc, T. Apih, J. Dolinšek, M. Šprogar, and B. Zalar

J. Stefan Institute, University of Ljubljana, 61000 Ljubljana, Slovenia

(Received 30 March 1995; revised manuscript received 18 July 1995)

The orientational glass transition in a $(NH_4I)_{0.44}(KI)_{0.56}$ single crystal has been studied by two-dimensional quadrupole perturbed ^{14}N NMR spectroscopy and ^{14}N spin-lattice relaxation time T_1 measurements. A ^{14}N T_1 minimum was found at 9 K. The ^{14}N inhomogeneous linewidth starts to increase strongly with decreasing T already below 50 K, i.e., on the high-temperature side of the T_1 minimum, demonstrating a breaking of the local cubic symmetry and the onset of the orientational glass transition in the fast motion regime. The ^{14}N magnetization recovery also changes from monoexponential to stretched-exponential below 50 K due to the development of spatial inhomogeneities in the sample as a result of a local glassy freeze-out. Both effects can be described by the presence of a local polarization distribution function $W(p)$ with a nonzero second moment M_2 below 50 K. The temperature dependence of the ^{14}N M_2, which is proportional to the Edwards-Anderson order parameter, shows that the glass transition is of the random-bond–random-field type. The random bond contribution is about three times stronger than the random-field one.

I. INTRODUCTION

It has been recently suggested that $(ND_4I)_{0.5}(KI)_{0.5}$ forms at low temperatures a dipolar orientational glass[1] of the random-bond type without the presence of random fields.[2] This is rather surprising since it is the presence of random fields[3] which distinguishes the transition in orientational glasses from the one in magnetic spin glasses.[4,5] In the absence of random fields the Sherrington-Kirkpatrick[6] (SK) model predicts that the Edwards-Anderson spin-glass order parameter

$$q_{EA} = \lim_{t\to\infty}\lim_{\Delta U\to\infty} [\langle S_i^z(0)S_i^z(t)\rangle]_{AV} = [\langle S_i^z\rangle^2]_{AV} \qquad (1)$$

is zero above the glass transition temperature T_G and nonzero below T_G:

$$q_{EA} = 0, \quad T > T_G \qquad (2a)$$

$$q_{EA} \neq 0, \quad T < T_G. \qquad (2b)$$

Here $\langle\cdots\rangle$ stands for the ensemble average and $[\cdots]_{AV}$ describes the disorder average. q_{EA}, which measures the mean-square local polarization, is thus the single valley glass order parameter obtained in the limit where the barriers ΔU between the different free-energy valleys diverge.[4] The presence of random fields in orientational glasses smears out the glass transition and induces a nonzero value of q_{EA} at any finite temperature.[3] In such a case an Almeida-Thouless (AT) line exists[3,7] in the temperature–random-field plane below which the SK solution becomes unstable and one has at low temperature a nonergodic spin-glass phase with an infinite number of order parameters, i.e., q_{EA} is replaced by an order-parameter function. At the AT line the field-cooled and zero-field-cooled susceptibilities should split and the maximum relaxation time should diverge. It should be however stressed that the above mean-field results are appropriate in the limit of infinite dimensions and that it is still open whether the above unusual properties will exist in three dimensions[7] also.

The predicted random-field smearing of the orientational glass transition has been observed in proton glasses by NMR.[8] Here the local freeze-out parameter q_{EA} has been determined from the second moment M_2 of the quadrupole perturbed Zeeman absorption line.[8] Alternatively the extent of the local freeze-out and the resulting spatial inhomogeneity can be also determined[2] from the deviation of the nuclear magnetization recovery from the monoexponential form predicted for a homogeneous sample.[9]

$(NH_4I)_x(KI)_{1-x}$ has been previously investigated by dielectric,[1] deuteron NMR,[2] inelastic neutron-scattering,[10,11] and Raman-scattering techniques.[12,13] The high-temperature plastic α phase has similarly as pure NH_4I the NaCl structure and changes close to $x = 1$ with decreasing temperature to the CsCl-type β phase where the NH_4^+ groups are dynamically disordered between two energetically equivalent orientations. At still lower temperatures the β phase changes into the orientationally ordered γ phase with a tetragonally deformed CsCl structure. For $0.7 < x < 0.95$ the α phase changes at lower temperatures into the β phase. For $0.55 < x < 0.7$ the α phase changes on cooling into a newly discovered[14] long-range ordered ε phase with trigonal symmetry $(R3m)$.

In the plastic α phase the NH_4^+ groups reorient in the octahedral environment between the eight $\langle 111\rangle$ axes. One N-H bond is assumed to point along the cube diagonals whereas the other ones are oriented towards the neighboring I^- ions. From this inequivalence a deformation of the NH_4^+ tetrahedra is expected to occur which may be accompanied by an off-center shift of the center of mass of the ion from its face-centered position. Considering the coupling between reorientations and distortions there are two possible types of reorientational movement. In the first case the reorientation is accompanied by a simultaneous change of distortion in the molecular frame so that the NH_4^+ group retains its shape in the crystal frame. Alternatively, rotations and distortions can be coupled so that the NH_4^+ group rotates as a rigid body.

For $x \lesssim 0.55$ no macroscopic symmetry change takes place[10] but a glasslike orientational freezing—driven by site

disorder and frustrated anisotropic dipole-dipole interactions[1,10]—occurs at low temperatures for $x > 0.2$. The distorted NH_4^+ ion was found to exhibit a nonzero electric dipole moment[1] of ≈ 1.4D suggesting that $(NH_4I)_x(KI)_{1-x}$ is a dipolar glass at low temperatures. Local antiferroelectric short-range ordering[10] of the NH_4^+ groups below $T = 50$ K further supports this model. For $x < 0.2$ single ion freezing has been reported to occur.[10]

The distortions of the NH_4^+ tetrahedra generate a nonzero electric-field gradient (EFG) tensor at the ^{14}N site, making it possible to detect the local deviations from the average cubic structure via a quadrupole-perturbed shift of ^{14}N NMR spectra. One should however have in mind that protons in the NH_4 molecule are indistinguishable so that only reorientations of NH_4^+ groups coupled with a change of the orientation of the EFG tensor with respect to the external magnetic field can be detected by NMR. In order to check on the nature of the glass transition in $(NH_4I)_x(KI)_{1-x}$ with $x = 0.44$ and more specifically, on the absence or presence of random fields in this system, we decided to measure the ^{14}N quadrupole perturbed NMR spectra as well as the ^{14}N magnetization recovery and spin-lattice relaxation time as a function of temperature. We also wished to compare the dynamics of $(NH_4I)_x(KI)_{1-x}$ with the one in $(ND_4I)_x(KI)_{1-x}$ (Ref. 2) in order to check on the possible tunneling of the NH_4^+ ions and the effect of quantum fluctuations on the glass transition.

II. EXPERIMENTAL

The Fourier transform ^{14}N solid echo NMR spectra and two-dimensional (2D) "separation of interactions" spectra[15] of a $(NH_4I)_{0.44}(KI)_{0.56}$ single crystal have been measured in a magnetic field of 6.34 T between 4.2 and 300 K. The ^{14}N spin-lattice relaxation time was measured by the $180° - \tau -$ solid echo-pulse sequence. The 90° pulse length was 9 μs. The sample composition has been checked by chemical analysis.

III. RESULTS

A. ^{14}N magnetization recovery and spin-lattice relaxation

The normalized magnetization recovery curves $M(t) = [I(0) - I(t)]/[I(0) - I(\infty)]$ recorded for different delay times t between 180° and the 90° pulses are presented in Fig. 1. At high temperatures the magnetization recovery is exponential,

$$M(t) = \exp(-t/T_1)$$ (3a)

yielding a single T_1 as expected for a $I = 1$ nucleus. At temperatures lower than 50 K deviations from the monoexponential recovery law occur which become stronger with decreasing temperatures in agreement with the behavior (Ref. 2) observed for deuteron spin-lattice relaxation in $(ND_4I)_{0.5}(KI)_{0.5}$. Such a behavior has been described[2] by a stretched-exponential magnetization recovery function
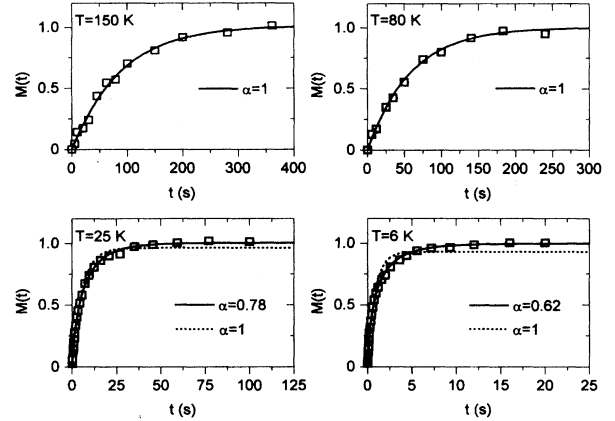
$$M(t) = \exp[-(t/T_1)^\alpha],$$ (3b)

FIG. 1. Magnetization recovery curves $M(t) = [I(0) - I(t)]/[I(0) - I(\infty)]$ in $(NH_4I)_{0.44}(KI)_{0.56}$ at different temperatures showing the gradual transition from monoexponential to a stretched-exponential relaxation behavior.

where $0 \leq \alpha \leq 1$. The stretched-exponential form of $M(t)$ demonstrates[2] the presence of a distribution $G(T_1)$ of spin-lattice relaxation times T_1 so that

$$M(t) = \int_0^\infty G(T_1)\exp(-t/T_1)dT_1.$$ (4)

As noted in Ref. 2 for fast motions where $\tau^{-1} \gg \omega_L$ the relaxation rate is always given by

$$T_1^{-1} = A\omega_Q^2\tau.$$ (5)

Here ω_Q is the fluctuating part of the ^{14}N quadrupole coupling and ω_L the nuclear Larmor frequency. A is a constant of the order of unity. In the slow motion limit expression (5) is generalized to $T_1^{-1} = f(\tau)$. The distribution of T_1^{-1} values $\tilde{G}(T_1^{-1})$ is in both limits related to the distribution of τ values $P(\tau)$ which is again related to the distribution of local barriers hindering $-NH_4^+$ reorientations and thus to the distribution of local polarizations $W(p)$.

The temperature dependence of the ^{14}N spin-lattice relaxation time T_1, as defined by Eq. (3b), is shown in Fig. 2 together with the temperature dependence of the "stretched" exponent α. The T_1 versus $10^3/T$ plot exhibits an asymmetric non-BPP-type[8] (Bloembergen-Purcell-Pound) minimum where $\omega_L\tau = 1$ at 9 K. This demonstrates that even in the glassy regime $\omega_L\tau \ll 1$ above 9 K so that the "fast motion" assumption[5] used in expression (5) is justified. The flattening out of the T_1 versus $10^3/T$ curve at the low-T side of the T_1 minimum seems to demonstrate the importance of tunneling processes in NH_4^+ group reorientations at low temperatures. In this connection it should be noted that the deuteron T_1 in $(ND_4I)_{0.5}(KI)_{0.5}$ exhibits[1] a T_1 minimum due to ND_4^+ reorientations at 12 K. The shift of the T_1 minimum from 9 to 12 K on deuteration shows that the ND_4^+ hindered rotation is significantly slower than the NH_4^+ one and demonstrates the importance of tunneling. Below 9 K $(NH_4I)_{0.44}(KI)_{0.56}$ is thus a quantum dipolar glass.
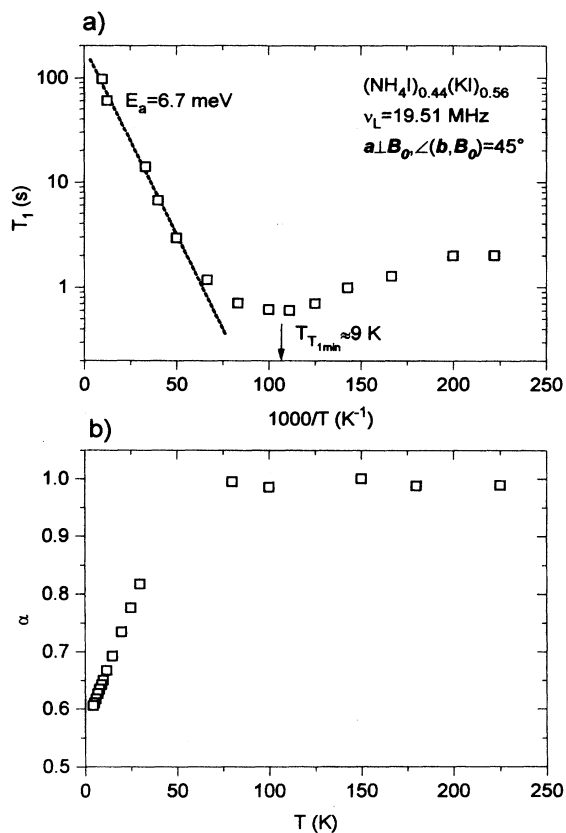
FIG. 2. (a) Temperature dependence of the [14]N T_1 defined by Eq. (3b). (b) Temperature dependence of the stretched exponent α.

B. NMR spectra

The temperature dependence of the ^{14}N NMR spectra is shown in Fig. 3. No well resolved ^{14}N quadrupole splitting into a doublet—as expected for a $I=1$ nucleus in a noncubic environment—is seen between 300 and 4.2 K. This demonstrates that the ^{14}N quadrupole coupling in the distorted NH_4^+ group is to a great extent motionally averaged out due to fast reorientations of the NH_4^+ group. The motional averaging is however not complete so that the NH_4^+ reorientations are not completely isotropic. The width of the ^{14}N NMR line varies with orientation (Fig. 4). The two-dimensional (2D) ^{14}N separation of interactions spectra[14] at 5 K (Fig. 5) show that the width of the inhomogeneous ^{14}N spectra—dominated by quadrupole interactions—is of the order of 40 kHz whereas the homogeneous width—dominated by nuclear dipolar coupling—is of the order of 500 Hz. The homogeneous linewidth remains nearly constant within the whole range of investigated temperatures. This demonstrates the presence of a local breaking of the cubic site symmetry and the resulting nonzero value of the local ^{14}N quadrupole coupling. The inhomogeneous broadening is compatible with the proposed C_{3v} symmetry of the distorted NH_4^+ ion and a displacement of the ^{14}N nuclei from the cubic sites. This effect becomes huge below 50 K. The inhomogeneous broadening is however significantly larger than the homogeneous one already at 200 K indicating the presence of random local strains.
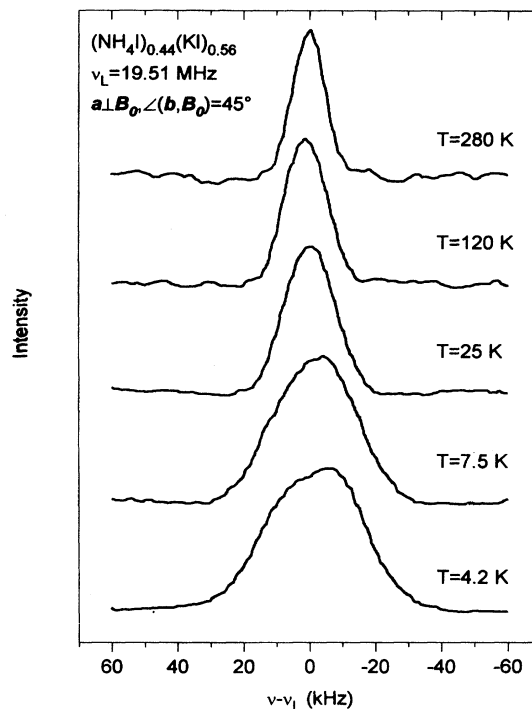

FIG. 3. Temperature dependence of the ^{14}N NMR line shapes in $(NH_4I)_{0.44}(KI)_{0.56}$ at an orientation $a\perp B_0, \angle(b,B_0)=45°$.

In $(NH_4I)_{0.44}(KI)_{0.56}$ we thus deal with a typical inhomogeneous ^{14}N frequency distribution $f(\nu)$ which is characteristic for orientational glasses and which reflects the distribution of local polarizations $W(p)$ of the NH_4^+ ions via[7]

$$f(\nu)d\nu = W(p)dp. \tag{6}$$

$W(p)$ is here defined by[2,3,7]

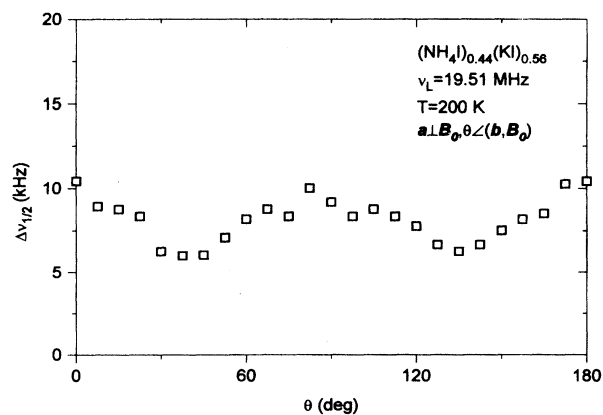$$W(p) = \frac{1}{N}\sum_i \delta(p - \langle S_i^z\rangle) = [\delta(p - \langle S_i^z\rangle)]_{AV}, \tag{7}$$

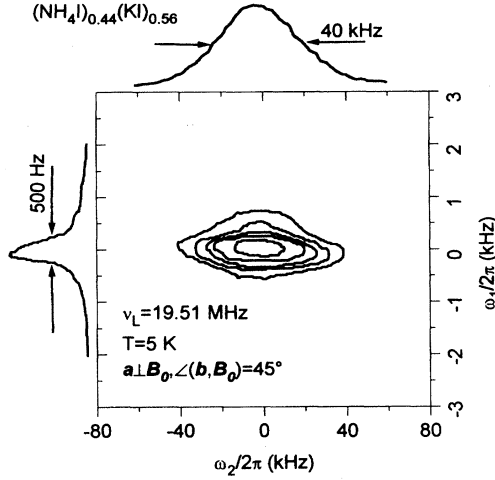FIG. 4. Angular dependence of the width of the ^{14}N NMR lines in $(NH_4I)_{0.44}(KI)_{0.56}$ at $T=200$ K.

FIG. 5. 2D ^{14}N "separation of interactions" (Ref. 15) NMR spectrum of $(NH_4I)_{0.44}(KI)_{0.56}$ at $T=5$ K. The solid echo $90°_x - t_1/2 - 90°_y - t_1/2 - S(t_1, t_2)$ pulse sequence was applied to obtain the 2D $I(\omega_1, \omega_2)$ spectrum after double-Fourier transforming the echo signal $S(t_1, t_2)$. The inhomogeneous linewidth is shown in the ω_2 and the homogeneous one in the ω_1 domain.

where we assume that the pseudospin S_i^z describes $C_{3\nu}$ orientations of the distorted NH_4^+ group[10] and $\langle \cdots \rangle$ stands for the ensemble average. For $C_{3\nu}$ symmetry the threefold symmetry axis of the NH_4^+ group is also the largest principal axis of the axially symmetric EFG tensor at the ^{14}N site and different orientations of this axis with respect to the external magnetic field will generally correspond to different ^{14}N quadrupole perturbed NMR frequencies. Here we also assumed that we are in the fast motion limit where the NH_4^+ reorientation time τ is much shorter than the characteristic NMR observation time,

$$\tau \ll (2\pi \Delta \nu_{\text{rigid lattice}})^{-1}. \tag{8}$$

Here $\Delta \nu_{\text{rigid lattice}}$ is $\approx 10^4 - 10^5$ Hz.

In such a case the NMR probe "sees" the time-averaged value of the EFG tensor and the pseudospin variable

$$p_i = \langle S_i^z \rangle \neq 0, \tag{9}$$

so that the local NMR frequency ν_i can be related to the local polarization in the linear approximation as

$$\nu_i = \nu_0 + \nu_1 p_i. \tag{10}$$

Since the Edwards-Anderson order parameter[4] $q_{\text{EA}} = [\langle S_i^z \rangle^2]_{\text{AV}}$ is just the second moment of $W(p)$,

$$q_{\text{EA}} = \int_{-1}^{1} W(p) p^2 dp, \tag{11a}$$

the second moment M_2 of the inhomogeneous frequency distribution $f(\nu)$ directly reflects the temperature dependence of q_{EA}:

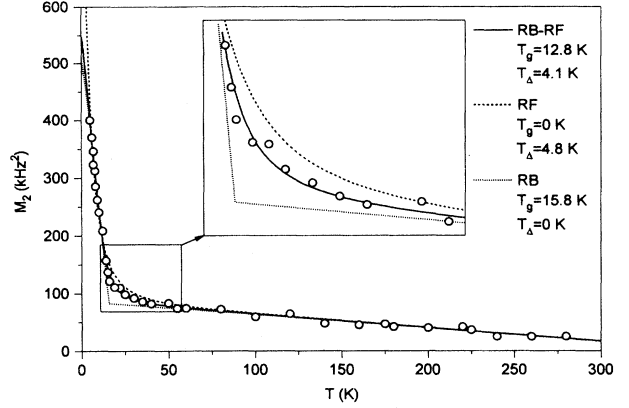$$M_2(q_{\text{EA}}) = \int_{-\infty}^{+\infty} f(\nu)(\nu - \nu_0)^2 d\nu = \nu_1^2 q_{\text{EA}}, \tag{11b}$$

FIG. 6. Temperature dependence of the second moment M_2 in $(NH_4I)_{0.44}(KI)_{0.56}$. The solid line represents the best fit to the RB-RF model, the dashed line the best fit to the RF model and the dotted line the best fit to the RB model. Obviously only the RB-RF model reproduces the observed curvature in the M_2 vs T plot.

as long as we are in the fast motion limit [Eq. (8)].

The temperature dependence of M_2 is presented in Fig. 6. The data in Fig. 6 show that M_2, and thus q_{EA}, is nonzero already at 300 K. Between 300 and 50 K M_2 increases linearly with decreasing temperature. This variation can be accounted for by thermal expansion enhanced by the presence of temperature-dependent random local strains.[16] The second moment strongly increases with decreasing temperatures below 50 K, i.e., in the fast motion regime on the high-temperature side of the T_1 minimum. The smearing out of the M_2 versus T curve shows that random fields must be present in addition to random bonds.

IV. DISCUSSION

Let us now first try to relate the ^{14}N magnetization recovery and the ^{14}N second moment data. We assume that, in addition to other reorientational degrees of freedom, the distorted NH_4^+ group is moving between several different $C_{3\nu}$ equilibrium orientations. The local electric-field gradient (EFG) tensor fluctuations $V_{\alpha\beta}(t)$ due to this motion are related to the local polarization fluctuations $p(t)$ via

$$V_{\alpha\beta}(t) = C_{\alpha\beta}\, p(t). \tag{12}$$

The autocorrelation function of $p(t)$ is

$$G_p(\tau) = \langle p(0)p(\tau) \rangle. \tag{13}$$

Without specifying the exact form of $G_p(\tau)$ we know that it is proportional to $(1 - p^2)$ and decays with a polarization-dependent correlation time $\tau_c(p)$.

The spectral density of $G_p(\tau)$,

$$J_p(\omega) = \int_0^{+\infty} G_p(\tau) e^{i\omega\tau} d\tau, \tag{14}$$

now determines the ^{14}N spin-lattice relaxation time

$$T_1^{-1}(p) \propto J_p(\omega), \tag{15}$$

which in turn depends on the local polarization p.

For an ensemble of NH_4^+ groups with a given local polarization p we find from the rate equations for the populations of the quadrupole-perturbed Zeeman states for the $I=1$ nucleus an exponential magnetization decay

$$M(t,p) \propto \exp[-(t/T_1(p))],\qquad (16)$$

if at $t=0$ both the $1 \rightarrow 0$ and $0 \rightarrow -1$ transitions are saturated. It is important to note that this form of $M(t,p)$ is independent of the specific form of the time decay of $G_p(\tau)$.

Since the glassy system is characterized by a local polarization distribution function $W(p)$, which introduces an inhomogeneity into the sample, $M(t,p)$ has to be averaged over $W(p)$:

$$\langle M(t) \rangle_G \propto \int_{-1}^{1} M(t,p)W(p)dp.\qquad (17)$$

For the random-bond—random-field (RB-RF) pseudospin Ising model with $S_i^z = \pm 1$ the calculation can be performed explicitly. The RB-RF Hamiltonian is here given by

$$H = -\sum_{ij} J_{ij} S_i^z S_j^z - \sum_i f_i S_i^z,\qquad (18)$$

where the J_{ij} are infinitely ranged quenched random interactions and f_i quenched random fields characterized by their second cumulants[3] $[J_{ij}^2]_{AV} = J^2/N$ and $[f_i f_j]_{AV} = \Delta \delta_{ij}$, respectively. If $f_i = 0$ we have a pure random-bond (RB) model, whereas we have a pure random-field (RF) case if $J_{ij} = 0$.

$W(p)$ is for the RB-RF case given[8] by

$$W(p) = \frac{1}{\sqrt{2\pi Q^2}} \frac{1}{1-p^2} \exp\left[-\frac{\mathrm{arctanh}^2 p}{2Q^2}\right],\qquad (19a)$$

where

$$Q = \sqrt{q_{EA}(T_g/T)^2 + (T_\Delta/T)^2}\qquad (19b)$$

increases with decreasing T. Here $T_g = J/k_B$ and $T_\Delta = \sqrt{\Delta}/k_B$.

$\langle M(t) \rangle_G$ can be now explicitly expressed as

$$\langle M(t) \rangle_G \propto \int_{-1}^{1} \exp\left[-\frac{t\sqrt{1-p^2}}{T_1(p=0)}\right] \frac{1}{1-p^2} \exp$$

$$\left[-\frac{\mathrm{arctanh}^2 p}{2Q^2}\right] dp.\qquad (20)$$

The above expression thus gives the desired relation between the dynamic quantities, i.e., the form of the ^{14}N magnetization recovery (which can be phenomenologically described by a stretched exponent), and the static quantities, i.e., the second moment of the ^{14}N NMR absorption line from which the Edwards-Anderson order parameter q_{EA} and random-bond—random-field parameters T_g and T_Δ (Refs. 3 and 8) can be determined.

The effective correlation time $\tau_c(p)$ for the transitions between two equilibrium orientations $A \rightarrow B$ and $B \rightarrow A$ is here given by

$$\frac{1}{\tau_c(p)} = W_{AB} + W_{BA} = 2\Omega_0 \cosh[U/2k_BT] = \frac{2\Omega_0}{\sqrt{1-p^2}},\qquad (21)$$

where $W_{AB} = \Omega_0 \exp[U/2k_BT]$ and $W_{BA} = \Omega_0 \exp[-U/2k_BT]$. Here U is the asymmetry of the double-well potential, $\Omega_0 = \tau_\infty^{-1} \exp[-E_a/k_BT]$ is the jump frequency, and E_a is the activation energy, respectively, barrier height in a symmetric double well. For a system with more than two equilibrium orientations the calculations are more complicated but qualitatively the results are similar.[17]

The magnetization decay is purely exponential only for

$$W(p) = \delta(p - P),\qquad (22)$$

i.e., for perfect long-range order or for $P=0$, i.e., in the paraelectric phase. The nonexponential form of $\langle M(t) \rangle_G$, Eq. (20), can be now phenomenologically described by a stretched-exponential form of the decay [Eq. (3b)]. As q_{EA} is the second moment of $W(p)$ it is clear that we find $\alpha = 1$, i.e., an exponential decay of $\langle M(t) \rangle_G$, only if Eq. (22) is fulfilled and the local polarization distribution is reduced to a δ function. Any broadening of $W(p)$—as expected for a glass transition—will lead to a value of α less than 1. The exact relation between α and Q has to be determined numerically. It should be stressed that the above general conclusions are not changed even in the case that there are more than two equilibrium orientations for the reorientable dipole determining $W(p)$.[17]

If one describes the temperature dependence of the T_1, which is here an effective parameter given by the fit of Eq. (3b) to the experimental data, in $(NH_4I)_{0.44}(KI)_{0.56}$ by the BPP formula

$$T_1^{-1} = A\omega_Q^2 \frac{\tau_c}{1+\omega^2\tau_c^2} + B\omega_Q^2 \frac{\tau_c}{1+4\omega^2\tau_c^2},\qquad (23)$$

where A and B are constants of the order of unity, one can extract from the data the correlation time $\tau_\infty = 9.4 \times 10^{-10}$ s as well as the activation energy $E_a = 6.7$ meV.

The stretched exponent α increases nearly linearly with increasing T between 4 K, where $\alpha = 0.6$, and 30 K, where $\alpha = 0.84$. At higher temperatures the increase in α is more gradual. At 100 K, $\alpha = 0.93$ and approaches 1 at and above 150 K. The temperature dependence of α, which reflects the inhomogeneous local freeze-out of the NH_4^+ dipoles on the $T_1 \approx 0.1$ s time scale, thus shows the same onset of the glass transition as the temperature dependence of the second moment of the ^{14}N NMR spectra.

The observed T dependence of M_2 is evidently due to two different processes. The low-temperature part reflects the onset of the glass transition as given by Eqs. (11a), (11b), (19a), and (19b), whereas the linear variation of M_2 with decreasing temperature between 300 and 50 K is evidently due to thermal expansion in the presence of random local strains. We thus have

$$M_2 = M_2(q_{EA}) + M_{2,\mathrm{lattice}}(T),\qquad (24)$$

where $M_{2,\mathrm{lattice}}(T)$ is a linear function of temperature.

Figure 6 shows the best fits of the experimentally observed temperature dependence of the $M_2 = M_2(T)$ to Eq. (24) for the RB-RF model, the RF model and the RB

model. Only the RB-RF model reproduces the observed curvature in the M_2 vs T plot at $T \approx 25$ K (see the enlarged inset to Fig. 6), yielding $T_g = 12.8$ K and $T_A = 4.1$ K. The value of $\nu_1 = 21.4$ kHz [Eq. (11b)] can be checked by extrapolating

$M_2(T)$, as obtained in the fast motion limit, to $T = 0$ K where $q_{EA} = 1$. The glass transition in $(NH_4I)_{0.44}(KI)_{0.56}$ is thus dominated by random bonds, though random fields are present also.

[1] I. Fehst, R. Böhmer, W. Ott, A. Loidl, S. Haussühl, and C. Bostoen, Phys. Rev. Lett. **64**, 3139 (1990).

[2] R. Böhmer, F. Fujara, and G. Hinze, Solid State Commun. **86**, 183 (1993).

[3] R. Pirc, B. Tadić, and R. Blinc, Phys. Rev. B **36**, 8607 (1987).

[4] K. Binder and A. P. Young, Rev. Mod. Phys. **58**, 801 (1986).

[5] S. F. Edwards and P. W. Anderson, J. Phys. F **5**, 965 (1973).

[6] D. Sherrington and S. Kirkpatrick, Phys. Rev. Lett. **35**, 1972 (1975).

[7] R. L. de Almeida and D. J. Thouless, J. Phys. A **11**, 983 (1978); R. F. Soares, F. D. Nobre, and J. R. L. de Almeida, Phys. Rev. B **50**, 6151 (1994).

[8] R. Blinc, J. Dolinšek, R. Pirc, B. Tadić, B. Zalar, R. Kind, and O. Liechti, Phys. Rev. Lett. **63**, 2248 (1989); R. Blinc, J. Dolinšek, V. A. Schmidt, and D. C. Ailion, Europhys. Lett. **6**, 55 (1988).

[9] A. Abragam, *The Principles of Nuclear Magnetism* (Oxford University Press, Oxford, 1960).

[10] J. F. Berret, C. Bostoen, J. L. Sauvajol, B. Hennion, and S. Haussühl, Europhys. Lett. **16**, 91 (1991); C. Bostoen, G. Coddens, and F. Wegener, J. Chem. Phys. **91**, 6337 (1989).

[11] R. Mukhopadhyay, J. Tomkinson, and C. J. Carlile, Europhys. Lett. **17**, 201 (1992).

[12] W. Joosen, H. Fleurent, C. Bostoen, and D. Shoemaker, Phys. Rev. B **43**, 11 542 (1991).

[13] J. F. Berret, F. Bruchäuser, R. Feile, C. Bostoen, and S. Haussühl, Solid State Commun. **74**, 1041 (1990).

[14] M. Paasch, M. Winterlich, R. Boehmer, R. Sonntag, G. McIntyre, and A. Loidl (private communication).

[15] J. Dolinšek, J. Magn. Reson. **92**, 312 (1992).

[16] T. Umeki, K. Yagi, and H. Terauchi, J. Phys. Soc. Jpn. **63**, 876 (1994).

[17] B. Tadić, R. Pirc, R. Blinc, J. Petersson, and W. Wiotte, Phys. Rev. B **50**, 9824 (1994).